The Schur Algorithm Applied to the One-Dimensional Continuous Inverse Scattering Problem

Youngchol Choi, *Member, IEEE*, Joohwan Chun, *Senior Member, IEEE*, Taejoon Kim, *Member, IEEE*, and Jinho Bae

***Abstract*—The one-dimensional continuous inverse scattering problem can be solved by the Schur algorithm in the discrete-time domain using sampled scattering data. The sampling rate of the scattering data should be increased to reduce the discretization error, but the complexity of the Schur algorithm is proportional to the square of the sampling rate. To improve this tradeoff between the complexity and the accuracy, we propose a Schur algorithm with the Richardson extrapolation (SARE). The asymptotic expansion of the Schur algorithm, necessary for the Richardson extrapolation, is derived in powers of the discretization step, which shows that the accuracy order (with respect to the discretization step) of the Schur algorithm is 1. The accuracy order of the SARE with the N-step Richardson extrapolation is increased to $N+1$ with comparable complexity to the Schur algorithm. Therefore, the discretization error of the Schur algorithm can be decreased in a computationally efficient manner by the SARE.**

***Index Terms*—Inverse scattering, reflection coefficient, Richardson extrapolation, Schur algorithm.**

I. Introduction

THE one-dimensional (1-D) inverse scattering problem (ISP) is to find the local reflectivity function of an inhomogeneous medium when the measurement for a known exciting signal at the boundary, called scattering data, are given. The examples for this classical 1-D ISP are inverse Schrödinger problem [1], [2], non-uniform transmission-line synthesis [3]–[5] and analysis [6]–[8], inverse acoustic scattering [9], [10], and seismic inversion problem [11], to list a few. The methodology to solve the 1-D ISP can be found in [12]–[15] and references therein. The Schur algorithm [14]–[16] is one of the most efficient methods for the 1-D ISP. Contrary to an integral equation method [17], the Schur algorithm does not have inner product in the recursion and is appropriate for parallel computation [14]. In addition, the Schur algorithm provides a fast Cholesky factorization method of Toeplitz matrices that have displacement structure, and the concept of displacement structure is generalized to some structured matrices [18]. Many researchers in various fields are motivated by this computationally efficient feature of the Schur algorithm, and the Schur algorithm is applied to many signal processing problems, including fast factorization of matrices [18]–[23], spectral factorization [24]–[27], filter design [28]–[36], estimation [37]–[41], digital communication [42]–[46], non-uniform transmission line synthesis [3], multidimensional BIBO stability test [47], underwater acoustics [48], and geophysics [49].

In general the scattering data is sampled at discrete time instants, and the 1-D continuous ISP (CISP) can be solved in the discrete time domain through the discretization of the governing equation. The discretized 1-D ISP becomes the identification problem of a uniformly layered medium whose reflection coefficients can be computed by the Schur algorithm. It is necessary to increase the sampling rate of the scattering data for the decrease of the discretization error. However, if the sampling rate is increased by a factor of n, the number of multiplications of the Schur algorithm are increased by a factor of n^2. To the best of author's knowledge, the fastest Schur algorithm has complextiy $O(8M(\log_2 M)^2)$ (see [18], [20] and references therein). Here, M is the number of layers. The computational gain of this fast Schur algorithm is obtained by the implementation of the Schur algorithm with a divide-and-conquer approach. But the complexity reduction is limited to large M and the advantage of parallel computation cannot be fully achieved.

The goal of this paper is to resolve this trade-off between the complexity and the accuracy. We propose a Schur algorithm with the Richardson extrapolation (SARE) as a numerically improved solution to the 1-D CISP. The key ingredient of the SARE is the Richardson extrapolation which accelerates the convergence of a numerical scheme that obeys an asymptotic expansion [50]–[52]. We derive the asymptotic expansion of the Schur algorithm through discretization error analysis carried out in two steps of the Schur algorithm: computation of the reflection coefficient and evolution of the wave variables. The Richardson extrapolation is made feasible by the derived asymptotic expansion, although the Richardson extrapolation procedure of the SARE is not straightforward because the SARE operates on the vector unlike the conventional numerical scheme based on the scalar. The SARE with the N-step

Manuscript received February 26, 2013; accepted April 05, 2013. Date of publication April 23, 2013; date of current version June 04, 2013. The associate editor coordinating the review of this manuscript and approving it for publication was Prof. Maria Sabrina Greco. This work was supported in part by the Ministry of Oceans and Fisheries of Korea under Grant D11205712H340000110. This paper was presented in part at International Conference on Acoustics, Speech, and Signal Processing, Philadelphia, PA, USA, March 2005.

Y. Choi is with Korea Institute of Ocean Science and Technology, Daejeon 305-343, Republic of Korea (e-mail: ycchoi@kiost.ac).

J. Chun is with the Department of Electrical Engineering, Korea Advanced Institute of Science and Technology (KAIST), Daejeon 305-701, Republic of Korea (e-mail: chun@ee.kaist.ac.kr).

T. Kim is with the Department of Electronic Engineering, City University of Hong Kong, Kowloon, Hong Kong (e-mail: taejokim@cityu.edu.hk).

J. Bae is with the Department of Ocean System Engineering, Jeju National University, Jeju 690-756, Republic of Korea (e-mail: baejh@jejunu.ac.kr).

Color versions of one or more of the figures in this paper are available online at http://ieeexplore.ieee.org.

Digital Object Identifier 10.1109/TSP.2013.2259487

Richardson extrapolation increases the accuracy of the Schur algorithm from $O(h)$ to $O(h^{N+1})$, where h is the discretization step. Nonetheless, the complexity of the SARE is comparable to the Schur algorithm.

Once the scattering data is gathered in an experiment, the accuracy of the Schur algorithm is fixed and cannot be enhanced, unless re-experiment is performed with the increased sampling rate. However, the proposed SARE can improve the accuracy without increasing the sampling rate, which is the most important result of this paper. Furthermore, any advanced methods for the Schur algorithm including divide-and-conquer and parallel computation, can be directly applied to the SARE for further improvement of the performance, because the SARE is a linear combination of the computation results of the Schur algorithm with different discretization steps. The SARE does not decrease the computational complexity of the Schur algorithm itself unlike the divide-and-conquer approach, but the computational efficiency of the SARE is achieved by exploiting the fundamental structures of the 1-D CISP itself.

The remainder of this paper is organized as follows. In Section II, the asymptotic expansion of the Schur algorithm is derived in powers of the discretization step. In Sections III and IV, we propose the SARE and numerical examples are provided to verify the theoritical results. Concluding remarks are given in Section V.

II. Asymptotic Expansion of the Schur Algorithm

A. Discretization of the 1-D CISP

The governing equations of the 1-D CISP are given by

$$\frac{\partial}{\partial x}\begin{bmatrix} W_R(x,t) \\ W_L(x,t) \end{bmatrix} = \begin{bmatrix} -\frac{\partial}{\partial t} & -k(x) \\ -k(x) & \frac{\partial}{\partial t} \end{bmatrix} \begin{bmatrix} W_R(x,t) \\ W_L(x,t) \end{bmatrix}, \quad (1)$$

where $W_R(x,t)$ and $W_L(x,t)$ are the right- and left-propagating waves, respectively, $k(x)$ is the local reflectivity function (LRF) at the position x, and t is the time variable. We try to find $k(x)$ when $W_R(0,t)$ and $W_L(0,t)$, called scattering data, are given. Without loss of generality, we assume that the time variable t is normalized such that the speed of the wave is 1. If the scattering data is sampled with the sampling period of $2h$, (1) needs to be discretized with the discretization step (DS) of h as follows [12],

$$\begin{bmatrix} W_R(x+h,t+h) \\ W_L(x+h,t-h) \end{bmatrix} = \frac{1}{\sqrt{1-(hk(x))^2}} \times \begin{bmatrix} 1 & -hk(x) \\ -hk(x) & 1 \end{bmatrix} \begin{bmatrix} W_R(x,t) \\ W_L(x,t) \end{bmatrix}. \quad (2)$$

The physical meaning of the discrete wave evolution equation (DWE) (2) can be explained using a lossless transmission-line model. The LRF $k(x)$ is defined by the impedance $Z(x)$ as follows

$$k(x) = \frac{Z'(x)}{2Z(x)}. \quad (3)$$

Assuming that h is sufficiently small, then

$$hk(x) = \frac{hZ'(x)}{2Z(x)} \approx \frac{h\left\{\frac{(Z(x)-Z(x-h))}{h}\right\}}{Z(x)+Z(x-h)} = \frac{Z(x)-Z(x-h)}{Z(x)+Z(x-h)}. \quad (4)$$

The above equation shows that $hk(x)$ can be interpreted as the reflection coefficient at the position x.

The Schur algorithm is a two-step recursive procedure. Assume that the medium is initially quiescent and the arrival time of the right-propagating wave at the position x is t.

Step 1) From the causality of the wave propagation,

$$W_L(x+h,\tau) = 0, \quad \tau < t+h. \quad (5)$$

Inserting (5) with $\tau = t-h$ into (2), $hk(x)$ is computed by

$$hk(x) = \frac{W_L(x,t)}{W_R(x,t)}. \quad (6)$$

Step 2) Use the DWE to find the wave variables at the position $x+h$.

B. Asymptotic Expansion

The continuously coupled interactions of the counter-propagating waves in the interval $[x, x+h)$ are converted to a single discrete reflector in the DWE, and this discretization process introduces the discretization error. An error analysis is performed for the two steps of the Schur recursion to derive the asymptotic expansion.

As can be seen in (4), $hk(x)$ is an approximation to the reflection coefficient. However, Step 1 of the Schur recursion computes the reflection coefficient using (6), which regards the approximated reflection coefficient $hk(x)$ as the exact instantaneous reflectivity at the position x. The following lemma identifies the numerical error of Step 1 of the Schur recursion by investigating the relation between $hk(x)$ and $\frac{W_L(x,t)}{W_R(x,t)}$.

Lemma 1: Assume that the arrival time of the right-propagating wave at the position x is t. If the LRF computed by (6) is denoted by $\tilde{k}(x)$, then

$$k(x) = \tilde{k}(x) + \sum_{n=1}^{\infty} \frac{W_L^{(n+1)}(x,t)}{(n+1)!W_R(x,t)} h^n, \quad (7)$$

where

$$W_L^{(n)}(x,t) = \left(\frac{\partial}{\partial x} - \frac{\partial}{\partial t}\right)^n W_L(x,t). \quad (8)$$

Proof: From the causality of the wave propagation, we get

$$W_L(x+h,t-h) = 0. \quad (9)$$

The Taylor series for $W_L(x+h,t-h)$ at (x,t) is given by

$$W_L(x+h,t-h) = W_L(x,t) + hW_L^{(1)}(x,t) + \sum_{n=2}^{\infty} \frac{W_L^{(n)}(x,t)}{n!} h^n. \quad (10)$$

From (1), we know that

$$W_L^{(1)}(x,t) = -k(x)W_R(x,t). \tag{11}$$

Inserting (9) and (11) into (10), (10) can be rewritten as

$$hk(x) = \frac{W_L(x,t)}{W_R(x,t)} + \sum_{n=2}^{\infty} \frac{W_L^{(n)}(x,t)}{n!W_R(x,t)} h^n. \tag{12}$$

Dividing both sides of (12) by h, we can obtain (7). □

Lemma 1 confirms the intuitive belief that $k(x)$ is closely related with $\frac{W_L(x,t)}{W_R(x,t)}$ which has the meaning of reflection. If the second term of the right hand side of (12) is regarded as error terms, $k(x)$ can be interpreted as density of the reflection coefficient. Note that $k(x)$ is a density function for the strength of the coupling of the counter-propagating waves. The reflection coefficient $hk(x)$ is an approximation for the integration of $k(x)$ over $[x-h, x)$. It is clear from (7) that Step 1 of the Schur recursion truncates the exact LRF at degree 0.

Step 2 of the Schur recursion evolves the wave variables using the DWE, assuming that the non-constant impedance of the interval $(x, x+h)$ is constant. Therefore, the waves computed by the DWE are not exact. The error due to these incorrect wave variables can be represented by a power series of h as shown in the following lemma.

Lemma 2: Assume that the arrival time of the right-propagating wave at the position x is t. Let us consider the one-step evolution of the Schur algorithm from x to $x+h$, assuming that $W_R(x,\tau)$ and $W_L(x,\tau)$ are known for all τ and $k(x)$ is known.

1) The right- and left-propagating waves computed by the DWE at $(x+h, t+h)$ are truncation at degree one of the Taylor series for the exact right- and left-propagating waves at (x,h) and $(x, t+2h)$, respectively.
2) If the LRF computed by (6) at $x+h$ using the wave variables computed by the DWE and the exact wave variables is denoted by $\hat{k}(x+h)$ and $\tilde{k}(x+h)$, respectively, then

$$\hat{k}(x+h) = \tilde{k}(x+h) + \sum_{n=1}^{\infty} a_n h^n, \tag{13}$$

where a_n is independent with h.

Proof: 1) From the DWE, we get

$$\hat{W}_R(x+h,t+h) = W_R(x,t) - hk(x)W_L(x,t) \tag{14}$$
$$\hat{W}_L(x+h,t+h) = W_L(x,t+2h) - hk(x)W_R(x,t+2h). \tag{15}$$

Here, the normalization factor $(1-(hk(x))^2)^{-1/2}$ is omitted for simplicity,[1] and the wave variables computed by the DWE are denoted by $\hat{W}_R$ and $\hat{W}_L$ which are different from the exact wave variables W_R and W_L. The Taylor series for $W_R(x+h, t+h)$ at (x,t) is given by

$$W_R(x+h,t+h) = W_R(x,t) + hW_R^{(1)}(x,t) + \sum_{n=2}^{\infty} \frac{W_R^{(n)}(x,t)}{n!} h^n, \tag{16}$$

[1]The normalization factor (NF) is important for energy conservation. However, this NF is a cofactor for all elements of a generator matrix. Therefore, the NF is canceled in Step 1 of the Schur algorithm (see (23)). Furthermore, the roundoff error of the Schur algorithm could be decreased if the reflection coefficient is computed without the NF.

where

$$W_R^{(n)}(x,t) = \left(\frac{\partial}{\partial x} + \frac{\partial}{\partial t}\right)^n W_R(x,t). \tag{17}$$

From (1), we know that

$$W_R^{(1)}(x,t) = -k(x)W_L(x,t). \tag{18}$$

Inserting (18) into (16), (16) is rewritten as

$$W_R(x+h,t+h) = W_R(x,t) - hk(x)W_L(x,t) + \sum_{n=2}^{\infty} \frac{W_R^{(n)}(x,t)}{n!} h^n. \tag{19}$$

Inserting (14) into (19), we get

$$W_R(x+h,t+h) = \hat{W}_R(x+h,t+h) + \sum_{n=2}^{\infty} \frac{W_R^{(n)}(x,t)}{n!} h^n. \tag{20}$$

It is clear from (20) that $\hat{W}_R(x+h,t+h)$ is truncation at degree one of the Taylor series for $W_R(x+h,t+h)$ at (x,t).

Similarly, the Taylor series for $W_L(x+h,t+h)$ at $(x,t+2h)$ is given by

$$W_L(x+h,t+h) = W_L(x,t+2h) + hW_L^{(1)}(x,t+2h) + \sum_{n=2}^{\infty} \frac{W_L^{(n)}(x,t+2h)}{n!} h^n. \tag{21}$$

Inserting (11) and (15) into (21), (21) is rewritten by

$$W_L(x+h,t+h) = \hat{W}_L(x+h,t+h) + \sum_{n=2}^{\infty} \frac{W_L^{(n)}(x,t+2h)}{n!} h^n. \tag{22}$$

Therefore, it is shown that $\hat{W}_L(x+h,t+h)$ is truncation at degree one of the Taylor series for $W_L(x+h,t+h)$ at $(x,t+2h)$.

2) We calculate $h\hat{k}(x+h)$ using (6) as follows

$$h\hat{k}(x+h) = \frac{\hat{W}_L(x+h,t+h)}{\hat{W}_R(x+h,t+h)} = \frac{W_L(x,t+2h) - hk(x)W_R(x,t+2h)}{W_R(x,t) - hk(x)W_L(x,t)}. \tag{23}$$

Inserting (20) and (22) into (23), we get

$$h\hat{k}(x+h) = \frac{W_L(x+h,t+h) - \sum_{n=2}^{\infty} \frac{W_L^{(n)}(x,t+2h)}{n!} h^n}{W_R(x+h,t+h) - \sum_{n=2}^{\infty} \frac{W_R^{(n)}(x,t)}{n!} h^n}. \tag{24}$$

Define

$$A = W_R(x+h,t+h), \tag{25}$$
$$B = \sum_{n=2}^{\infty} \frac{W_R^{(n)}(x,t)}{n!} h^n, \tag{26}$$
$$C = W_L(x+h,t+h), \tag{27}$$
$$D = \sum_{n=2}^{\infty} \frac{W_L^{(n)}(x,t+2h)}{n!} h^n. \tag{28}$$

If h is sufficiently small such that $\left|\frac{B}{A}\right| < 1$, then (24) can be rewritten as

$$\begin{aligned} h\hat{k}(x+h) &= \frac{C-D}{A-B} = \frac{1}{A}(C-D)\left(1-\frac{B}{A}\right)^{-1} \\ &= \frac{1}{A}(C-D)\left(1+\sum_{n=1}^{\infty}\left(\frac{B}{A}\right)^n\right) \\ &= \frac{C}{A}+\frac{C}{A}\sum_{n=1}^{\infty}\left(\frac{B}{A}\right)^n - \frac{D}{A}\sum_{n=0}^{\infty}\left(\frac{B}{A}\right)^n. \end{aligned} \quad (29)$$

It is obvious that the second and third term of (29) are power series of h, in which the minimum degree is two. Also, note that

$$\frac{C}{A} = \frac{W_L(x+h,t+h)}{W_R(x+h,t+h)} = h\tilde{k}(x+h). \quad (30)$$

Inserting (30) into (29), we obtain

$$h\hat{k}(x+h) = h\tilde{k}(x+h) + \sum_{n=2}^{\infty} a_{n-1}h^n. \quad (31)$$

Dividing both sides of (31) by h, we get (13). □

The physical meaning of the Schur algorithm is seen clearly in the first part of Lemma 2. The Schur algorithm computes the wave variables with accuracy $O(h^2)$ and the remained error term is represented by a familiar Taylor series expansion. In addition, the points of the Taylor series in (16) and (21) are time-delayed, (x,h), and time-advanced, $(x,t+2h)$, respectively, with respect to the target position $(x+h,t+h)$, which are in agreement with the time-delay and time-advance operation of the discretized wave evolution (2).

The asymptotic expansion of the Schur algorithm is reached by merging power series (7) and (13) in the following theorem.

Theorem 1: Under the same assumption as in Lemma 2, the asymptotic expansion of the LRF reconstructed by the one-step evolution of the Schur algorithm from x to $x+h$ is given by

$$\hat{k}(x+h) = k(x+h) + \sum_{n=1}^{\infty} c_n h^n, \quad (32)$$

where c_n is independent with h.

Proof: From Lemma 1, we know that

$$k(x+h) = \tilde{k}(x+h) + \sum_{n=1}^{\infty} \frac{W_L^{(n+1)}(x+h,t+h)}{(n+1)!W_R(x+h,t+h)}h^n. \quad (33)$$

Inserting (13) into (33), we get (32). □

It is easy to see that Theorem 1 also holds at any position by induction due to the recursive nature of the Schur algorithm. From (32), the accuracy of the Schur algorithm is $O(h)$.

In order to provide an intuition for the SARE, we give an illustrative example. We denote the LRF computed by the Schur algorithm with the DS of $h/2^i$ at the position x as $\hat{k}_{i,h}(x)$. From Theorem 1, we can write

$$\hat{k}_{i,h}(x) = k(x) + \sum_{n=1}^{\infty} c_n\left(\frac{h}{2^i}\right)^n. \quad (34)$$

The N-step Richardson extrapolation combines $\hat{k}_{i,h}(x)$, $i = 0,1,\cdots,N$, to eliminate $c_n(h/2^i)^n$ of (34), $n = 1,2,\cdots,N$, and thus, the accuracy is increased to $O(h^{N+1})$. For example, the 2-step Richardson extrapolation procedure is given by [52]

$$8/3\times\hat{k}_{2,h}(x) - 2\times\hat{k}_{1,h}(x) + 1/3\times\hat{k}_{0,h}(x) = k(x) + \sum_{n=3}^{\infty} c'_n h^n, \quad (35)$$

where c'_n is independent with h. It can be seen from (35) that the 2-step Richardson extrapolation increases the accuracy from $O(h)$ to $O(h^3)$. Note that the value of c_n in (32) is not necessary for the Richardson extrapolation. We present the N-step SARE with detailed numerical behaviors in the following section.

III. SARE

Using the Richardson extrapolation strategy based on the derived asymptotic expansion, we propose the N-step SARE that is a linear combination of the LRFs reconstructed by the Schur algorithm with the DSs of $\{h, h/2, \cdots, h/2^N\}$. The generator matrix $G_{N,h}$ for the smallest DS $h/2^N$ is given by

$$G_{N,h} = \begin{bmatrix} W_R\left(0,\frac{0}{2^N}\right) & W_L\left(0,\frac{0}{2^N}\right) \\ W_R\left(0,\frac{2h}{2^N}\right) & W_L\left(0,\frac{2h}{2^N}\right) \\ W_R\left(0,\frac{4h}{2^N}\right) & W_L\left(0,\frac{4h}{2^N}\right) \\ \vdots & \vdots \end{bmatrix}^T. \quad (36)$$

The LRF vector $\Theta_{i,h}$ is defined by

$$\Theta_{i,h} \triangleq \left[\hat{k}_{i,h}\left(\frac{0}{2^i}\right) \quad \hat{k}_{i,h}\left(\frac{h}{2^i}\right) \quad \hat{k}_{i,h}\left(\frac{2h}{2^i}\right) \quad \cdots\right]. \quad (37)$$

If we define a column-wise down-sampled matrix $F^{[d]}$ of a matrix F as

$$F^{[d]}(i,l) \triangleq F\left(i, d(l-1)+1\right), \quad (38)$$

$\Theta_{i,h}$ can be obtained by applying the Schur algorithm to $G_{N,h}^{[2^{N-i}]}$, where $F^{[d]}(i,l)$ and $F(i,l)$ are (i,l) element of $F^{[d]}$ and F, respectively. Note that $\Theta_{i,h}$ is the LRF computed by the Schur algorithm with the DS of $h/2^i$. Now, the LRF vector $K_{N,h}$ of the N-step SARE is obtained by the Richardson extrapolation procedure as follows

$$K_{N,h} = \sum_{i=0}^{N} \beta_{N,i}\Theta_{i,h}^{[2^i]}, \quad (39)$$

where $\beta_{N,i}$ is given by [52]

$$\beta_{N,i} = \frac{(-1)^{N-i}2^{i(i+1)/2}}{\left(\prod_{l=1}^{i}(2^l-1)\right)\times\left(\prod_{l=1}^{N-i}(2^l-1)\right)}. \quad (40)$$

The error terms of (34) whose degrees are smaller than $N+1$ are eliminated in (39), and the accuracy of the SARE is $O(h^{N+1})$.

At first glance (39) seems like the conventional Richardson extrapolation procedure, but it is important to adjust the position of $\Theta_{i,h}$. The N-step SARE requires the values of $\Theta_{i,h}$ for all i, $0 \le i \le N$, at a specific position. However, the reconstructed positions of $\Theta_{i,h}$, $qh/2^i$, $q = 0,1,2,\cdots$, are different for each i. To explain how the positions of $\Theta_{i,h}$ should be aligned, the 2-step SARE is depicted in Fig. 1 as an illustrative example. Because the reconstructed positions except for qh, indicated by

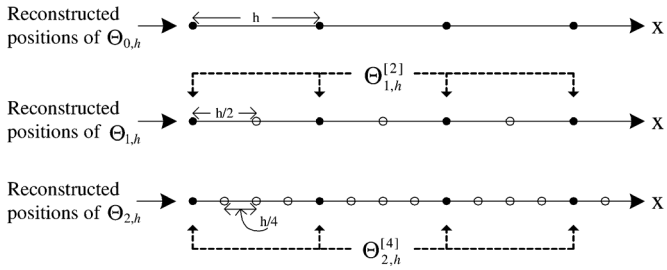

Fig. 1. Reconstructed positions of $\Theta_{i,h}$, $i = 0, 1, 2$, for the 2-step SARE.

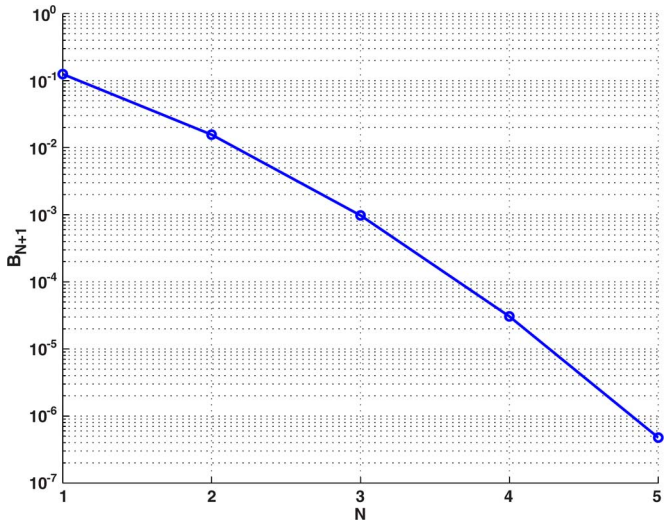

Fig. 2. B_{N+1} versus N.

open circle in Fig. 1, cannot be obtained by $\Theta_{0,h}$, the 2-step SARE can be executed only at qh, indicated by filled circle in Fig. 1. In general, the N-step SARE can be achieved only at multiples of h, where the positions of all $\Theta_{i,h}$, $0 \le i \le N$ are overlapped. This is why down-sampling $\Theta^{[2^i]}_{i,h}$ of $\Theta_{i,h}$ is performed in (39).

The lowest order term of the error terms in (39) can be expressed as follows

$$\underbrace{\sum_{i=0}^{N} \beta_{N,i} 2^{-i(N+1)}}_{=B_{N+1}} c_{N+1} h^{N+1}, \tag{41}$$

where $c_{N+1}h^{N+1}$ is the $(N+1)$th order term of the error terms for $\Theta_{0,h}$. For the accuracy order of the Schur algorithm to be equivalent with the N-step SARE, it is natural to decrease the DS of the Schur algorithm from h to h^{N+1}. In this case, the lowest order term of the error terms for the Schur algorithm is given by

$$c_1 h^{N+1}. \tag{42}$$

We plot B_{N+1} with respect to N in Fig. 2. Although it can not be determined whether (41) is greater than (42) or not,[2] it is worth of notice that B_{N+1} decays exponentially as seen in Fig. 2. This exponentially decaying behavior of B_{N+1} can provide considerable additional improvement of accuracy. The advantage of B_{N+1} can be observed in a numerical example at the end of this section.

[2]It is clear from the derivation procedure of the asymptotic expansion that we can not get any analytical information about c_i. Therefore, an analytical comparison between the N-step SARE and the Schur algorithm with the DS of h^{N+1} is generally unsuitable.

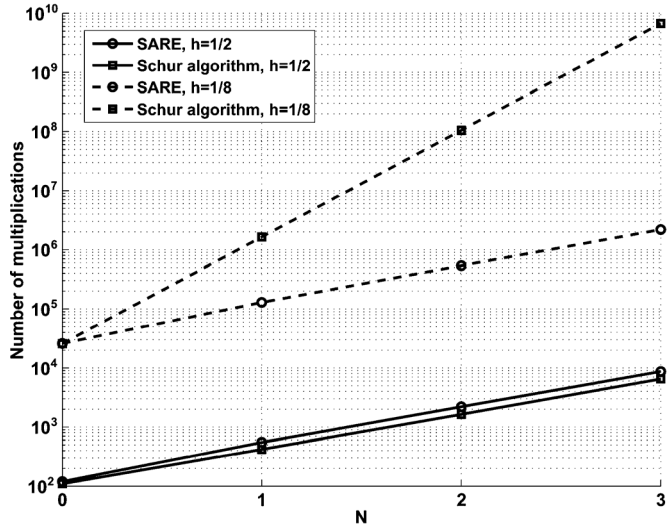

Fig. 3. Complexity vs. N for the SARE and the Schur algorithm when $h = 1/2$ and $h = 1/8$.

If it is necessary to identify a continuous medium at sparse positions instead of the exhaustive examination over the whole medium, the SARE can provide a computationally efficient solution. To be specific, assume that the target DS is h when the DS of the given scattering data is h^{N+1}. In this case, the N-step SARE is enough to get the accuracy that corresponds to the Schur algorithm with the given scattering data. If the number of layers with the DS of h is M, the N-step SARE requires

$$\sum_{i=0}^{N} \left((2^i M)^2 + 2^i M \right) + (N+1)M = \frac{(4^{N+1}-1)}{3} M^2 + (2^{N+1} + N)M \tag{43}$$

multiplications. Although we need the LRF only at multiples of h, the conventional Schur algorithm should be run using the given scattering data in order to preserve accuracy $O(h^{N+1})$, in which $\frac{M^2}{h^{2N}} + \frac{M}{h^N}$ multiplications are required. The complexity is compared as a function of N in Fig. 3, where $M = 10$ and $M = 40$ for $h = 1/2$ and $h = 1/8$, respectively. If logarithm is taken for the dominant M^2-term of the complexity, we get

$$\text{SARE} : \log \frac{(4^{N+1}-1)}{3} M^2 \approx N \log 4 + 2 \log M \tag{44}$$

$$\text{Schur} : \log \frac{M^2}{h^{2N}} = -2N \log h + 2 \log M. \tag{45}$$

The slope of (44) and (45) with respect to N are $\log 4$ and $-2 \log h$, respectively. These two slopes become equivalent when $h = 1/2$. However, the slope of the Schur algorithm logarithmically increases as h decreases and is larger than the constant slope of the SARE when $h < 1/2$. These observations can be clearly seen in Fig. 3. Therefore, the computational efficiency of the SARE is better revealed for small h. In the case of $h = 1/8$, the 3-step SARE reduces the complexity of the Schur algorithm by a factor of 3×10^3 as shown in Fig. 3.

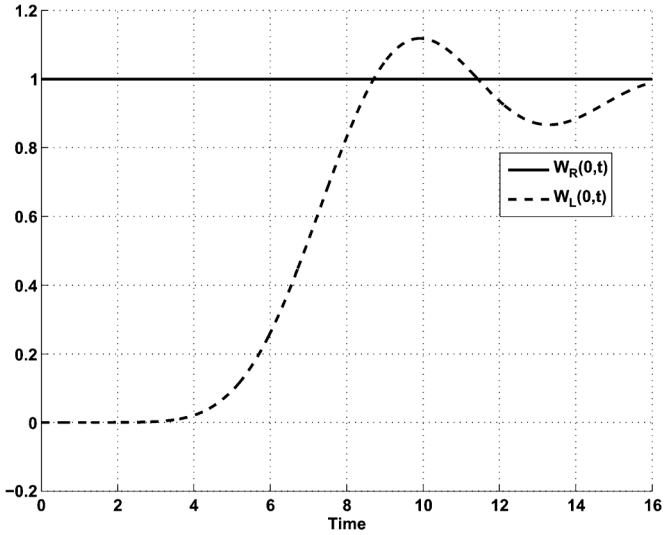

Fig. 4. Scattering data.

A. Simulation Example

To evaluate the discretization error of the SARE, it is desirable to use a case which has exact solution for a specific scattering data. So far the scattering data obtained from a rational transfer function is the only known example in which the exact LRF can be computed [36]. However, a numerical procedure should be performed to solve the characteristic polynomial except for the transfer function of Butterworth filter. Therefore, it is the best to utilize the scattering data generated by the transfer function of Butterworth filter. In addition, the step response of Butterworth filter is used as the scattering data in order to sidestep any approximation for the generation of the scattering data. The transfer function of an Lth order Butterworth filter with unit cutoff frequency can be expressed by

$$\frac{r}{\prod_{i=1}^{L}(s-p_{i,L})}=\frac{\sum_{i=1}^{L}c_{i,L}}{(s-p_{i,L})}, \tag{46}$$

where r is a constant, $p_{i,L}=\exp(j\pi/2)\exp(j(2i-1)\pi/2L)$, and $c_{i,L}=r/\prod_{n\neq i}(p_{i,L}-p_{n,L})$. In this simulation $W_R(0,t)$ is the unit step function of t and $W_L(0,t)$ is given by the step response of a 10th order Butterworth filter as follows

$$\begin{aligned}W_L(0,t)&=\int_0^t\sum_{i=1}^{10}c_{i,10}\exp(p_{i,10}\tau)d\tau\\&=\sum_{i=1}^{10}\frac{c_{i,10}}{p_{i,10}}\left(\exp(p_{i,10}t)-1\right).\end{aligned} \tag{47}$$

We fix r at 0.95. This scattering data is plotted in Fig. 4. For a quantitative comparison of the SARE with the Schur algorithm, the reconstruction error $e(x)$ and the normalized reconstruction error $\bar{e}$ are defined by

$$e(x)=\left|k(x)-\hat{k}(x)\right|, \tag{48}$$

$$\bar{e}=\frac{\int e(x)dx}{\int|k(x)|\,dx}, \tag{49}$$

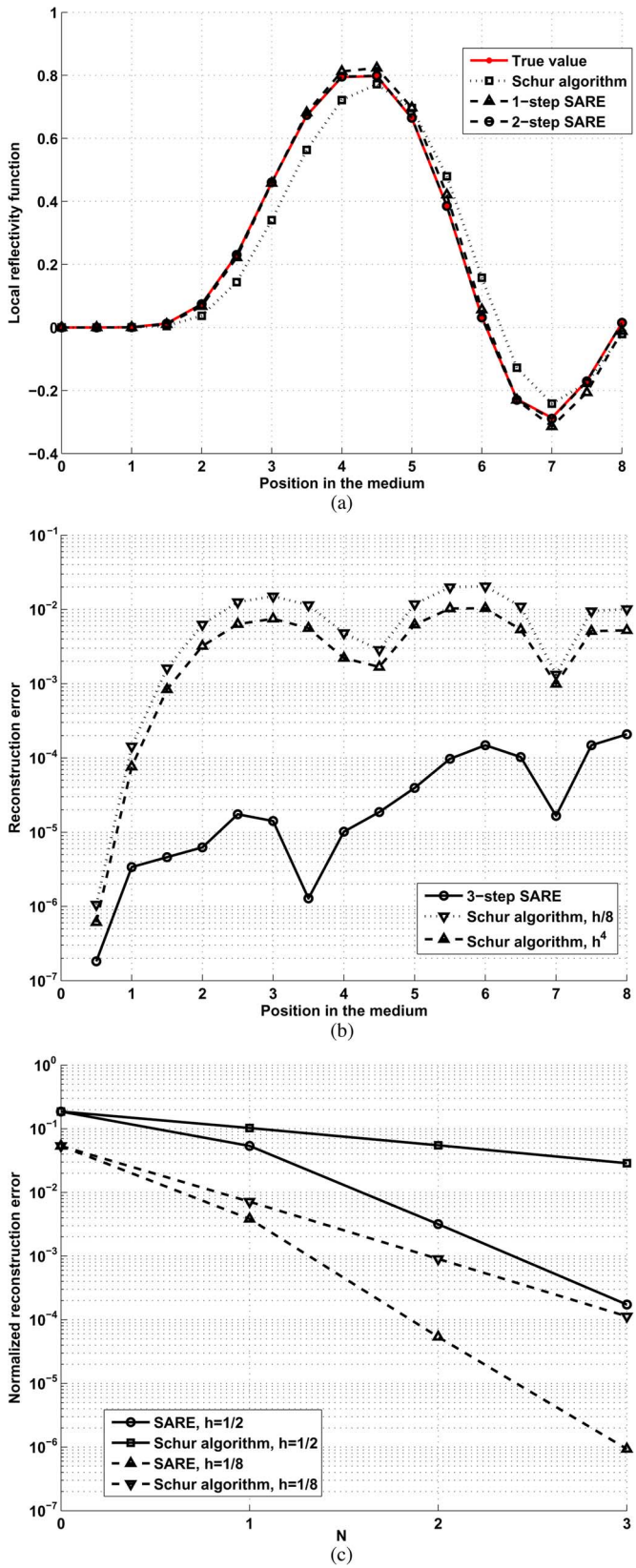

Fig. 5. Demonstration of the improved accuracy of the SARE: (a) reconstructed LRF for $h=1/2$, (b) reconstruction error of the 3-step SARE when $h=1/2$, (c) normalized reconstruction error versus N when $h=1/2$ and $h=1/8$.

where $k(x)$ is the true value of the LRF and $\hat{k}(x)$ is the reconstructed LRF.

In Fig. 5, we demonstrate the performance of the SARE up to 3-step case which was sufficient to show the superiority of the SARE over the Schur algorithm. The reconstructed LRFs for $h = 1/2$ are plotted in Fig. 5(a). It can be seen from Fig. 5(a) that the error of the Schur algorithm is decreased by the SARE as N increases, and the LRF of the 2-step SARE cannot be discriminated from the true value in this figure. The reconstruction error for the 3-step SARE is shown for $h = 1/2$ in Fig. 5(b). To verify the accuracy $O(h^4)$ of the 3-step SARE, the Schur algorithm with the DS of h^4 is also plotted in this figure. The Schur algorithm with the DS of $h/8$, which is the smallest DS in the 3-step SARE, is added in Fig. 5(b). It is clear from Fig. 5(b) that the reconstruction error of the 3-step SARE is remarkably smaller than the Schur algorithm with the DS of h^4 over the whole medium, which proves the accuracy order of the 3-step SARE and the value of exponentially decaying B_{N+1}. In Fig. 5(c), the normalized reconstruction error for $h = 1/2$ and $h = 1/8$ is illustrated with respect to N, which shows the accuracy of the SARE at a glance. For the same accuracy as the N-step SARE, the DS of the Schur algorithm in Fig. 5(c) is h^{N+1}. We can confirm in Fig. 5(c) that the accuracy of the N-step SARE is congruent or larger than the accuracy of the Schur algorithm with the DS of h^{N+1}. In addition, the accuracy improvement of the SARE becomes greater than the increased accuracy order as N increases. The shape of the graphs for $h = 1/2$ is identical to that for $h = 1/8$, because the ratio of the dominant term of the reconstruction error for the N-step SARE, $B_{N+1}c_{N+1}h^{N+1}$, to that for the Schur algorithm with the DS of h^{N+1}, $c_1 h^{N+1}$, is not dependent on h. However, the computational efficiency of the SARE is increased as h decreases. For example, the normalized reconstruction error of the 3-step SARE for $h = 1/8$ corresponds to that of the Schur algorithm with the DS of $\frac{1}{4} \times 10^{-5}$. The computational gain of the SARE amounts to 10^7 in this case.

IV. Extended SARE

The spacing of the reconstructed positions in Section III is h, even if the involved DSs are smaller than or equal to h. In this section, assuming that the DS of the given scattering data is h, we extend the N-step SARE (39) to get the LRF with the DS of h. Once the DS of the scattering data is fixed by the sampling rate, the DS that is lower than h is not available. Instead of the DSs of $\{h, h/2, \cdots, h/2^N\}$ in (39), we start from the N-step SARE with the DSs of $\{2^N h, 2^{N-1}h, \cdots, h\}$, which means down-sampling of the given scattering data by integer factor, as follows

$$K_{N,2^N h} = \sum_{i=0}^{N} \beta_{N,i} \Theta_{i,2^N h}^{[2^i]}. \tag{50}$$

The subscript of (39) is suitably altered in (50) according to the change of the involved DSs. As mentioned in Section III, the reconstructed positions of (50) are $q2^N h$, $q = 0, 1, 2, \cdots$. However, the DS of the given scattering data is h, not $2^N h$. In order to get a solution corresponding to the given scattering data, we change the initial position of (50) from 0 to mh, $m = 0, 1, \cdots, 2^N - 1$, and add one more subscript to denote this initial position mh as follows

$$G_{N,2^N h,m} = \begin{bmatrix} W_R(0,(2m)h) & W_L(0,(2m)h) \\ W_R(0,(2+2m)h) & W_L(0,(2+2m)h) \\ W_R(0,(4+2m)h) & W_L(0,(4+2m)h) \\ \vdots & \vdots \end{bmatrix}^T, \tag{51}$$

$$\Theta_{i,2^N h,m} = \begin{bmatrix} \hat{k}_{i,2^N h}(mh) \\ \hat{k}_{i,2^N h}\big((m+2^{N-i})h\big) \\ \hat{k}_{i,2^N h}\big((m+2\times 2^{N-i})h\big) \\ \vdots \end{bmatrix}^T. \tag{52}$$

Note that $\Theta_{i,2^N h,m}$ is computed by applying the Schur algorithm to $G_{N,2^N h,m}^{[2^{N-i}]}$. Now, the N-step SARE computes the LRF at $m + q2^N h$, $q = 0, 1, 2, \cdots$, as follows,

$$K_{N,2^N h,m} = \sum_{i=0}^{N} \beta_{N,i} \Theta_{i,2^N h,m}^{[2^i]}. \tag{53}$$

Therefore, if the N-step SARE is repeated 2^N-times which is the ratio of the largest DS $2^N h$ to the smallest DS h, we can obtain the LRF with the increased accuracy $O((2^N h)^{N+1})$.

The complexity of (53) can be decreased if we examine (52) carefully. If m is larger than or equal to 2^{N-i}, the reconstructed positions of $\Theta_{i,2^N h,m}$ overlap with $\Theta_{i,2^N h,\bar{m}}$, where

$$\bar{m} = m - \left\lfloor \frac{m}{2^{N-i}} \right\rfloor \times 2^{N-i},$$

and $\lfloor a \rfloor$ is the largest integer less than or equal to a. For example, we compare $\Theta_{1,8h,1}$ and $\Theta_{1,8h,5}$ as follows,

$$\Theta_{1,8h,1} = \begin{bmatrix} \hat{k}_{1,8h}(h) \\ \hat{k}_{1,8h}(5h) \\ \hat{k}_{1,8h}(9h) \\ \vdots \end{bmatrix}^T, \quad \Theta_{1,8h,5} = \begin{bmatrix} \hat{k}_{1,8h}(5h) \\ \hat{k}_{1,8h}(9h) \\ \hat{k}_{1,8h}(13h) \\ \vdots \end{bmatrix}^T, \tag{54}$$

which shows that $\Theta_{1,8h,5}$ is obtained by dropping the first element of $\Theta_{1,8h,1}$. In general, $\Theta_{i,2^N h,m}$, $m \geq 2^{N-i}$, is gained by removing the first m_i elements of $\Theta_{i,2^N h,\bar{m}}$, where

$$m_i = \left\lfloor \frac{m}{2^{N-i}} \right\rfloor.$$

Therefore 2^{N-i} executions of the Schur algorithm with the DS of $2^{N-i}h$ is enough. We call the detailed procedure of this section as the extended SARE (ESARE). The number of multiplications for the ESARE is

$$\sum_{i=0}^{N} 2^{N-i} \left(\left(\frac{M}{2^{N-i}} \right)^2 + \frac{M}{2^{N-i}} \right) < \sum_{i=-\infty}^{N} \left(\frac{M^2}{2^{N-i}} \right) + (N+1)M = 2M^2 + (N+1)M. \tag{55}$$

Only the multiplications associated with the computation of Θ are counted in (55) because the complexity of the rest is $O(M)$. If we compare the dominant M^2-term of (55) with that of the conventional Schur algorithm, the complexity of the ESARE

is less than twice of that of the Schur algorithm. That is, the complexity of the ESARE is comparable to the Schur algorithm although the accuracy order is increased from 1 to $N+1$. The complexity of (39) increases exponentially with respect to N as shown in (43), because the number of layers for each involved DS also increases exponentially. However, the complexity of the ESARE is almost independent on N due to the exponentially decreasing DSs and the avoidance of unnecessarily duplicated computations.

The Richardson extrapolation converges to the exact value as N tends to infinity if h_P/h_{P-1} is less than unity for all P, where h_P is the newly added DS in the P-step Richardson extrapolation [50], [51]. However, unlike the SARE, the newly added DS of the ESARE increases as N increases, and the convergence of the ESARE is not guaranteed. Therefore, the value of N can not be made arbitrarily large in the ESARE, and we need a stopping criteria for N. To this end, we consider the dominant term for the reconstruction error of the ESARE can be obtained by the replacement of h in (41) with $2^N h$, which is given by

$$B_{N+1}c_{N+1}(2^N h)^{N+1} = \underbrace{2^{N^2+N}B_{N+1}h^{N+1}}_{=Q_{N+1}}c_{N+1}. \quad (56)$$

From (40) and (41), we get

$$\begin{aligned}
|B_{N+1}| &= \left|\sum_{i=0}^{N}\beta_{N,i}2^{-i(N+1)}\right| \\
&= \left|\sum_{i=0}^{N}\frac{(-1)^{N-i}2^{i(i+1)/2}}{\left(\prod_{l=1}^{i}(2^l-1)\right)\times\left(\prod_{l=1}^{N-i}(2^l-1)\right)}2^{-i(N+1)}\right| \\
&\geq \left|\sum_{i=0}^{N}\frac{(-1)^{i}2^{i(i+1)/2}}{\left(\prod_{l=1}^{i}2^l\right)\times\left(\prod_{l=1}^{N-i}2^l\right)}2^{-i(N+1)}\right| \\
&= \left|\sum_{i=0}^{N}\frac{(-1)^{i}2^{i(i+1)/2}}{\left(2^{i(i+1)/2}\right)\times\left(2^{(N-i)(N-i+1)/2}\right)}2^{-i(N+1)}\right| \\
&= 2^{-(N^2+N)/2}\left|\sum_{i=0}^{N}(-1)^i 2^{-(i^2+i)/2}\right| \\
&\geq 2^{-(N^2+N)/2}. \quad (57)
\end{aligned}$$

As N increases, it is clear from (57) that $|Q_{N+1}|$ increases exponentially, and that the value of (56) can be significantly increased by Q_{N+1}. Therefore, if the unknown c_{N+1} is ignored in (56), the decreasing rate of the error of the ESARE can be considerably degraded by Q_{N+1} as N increases. On the other hand, $|Q_{N+1}|$ is a convex function with respect to N due to the monotonicity of $B_{N+1}h^{N+1}$ and 2^{N^2+N}. The magnitude of Q_{N+1} is shown in Fig. 6, in which convexity can be clearly seen. As a rule of thumb, we suggest that the maximum value of N, denoted by $N_{h,\max}$, is chosen by the integer value which minimizes $|Q_{N+1}|$.

Remark 1: The SARE or ESARE is a linear combination of the Schur algorithm, and the complexity is dominated by the complexity of the Schur algorithm. Therefore computationally efficient methods of the Schur algorithm can be directly employed to further decrease the complexity of the SARE or ESARE.

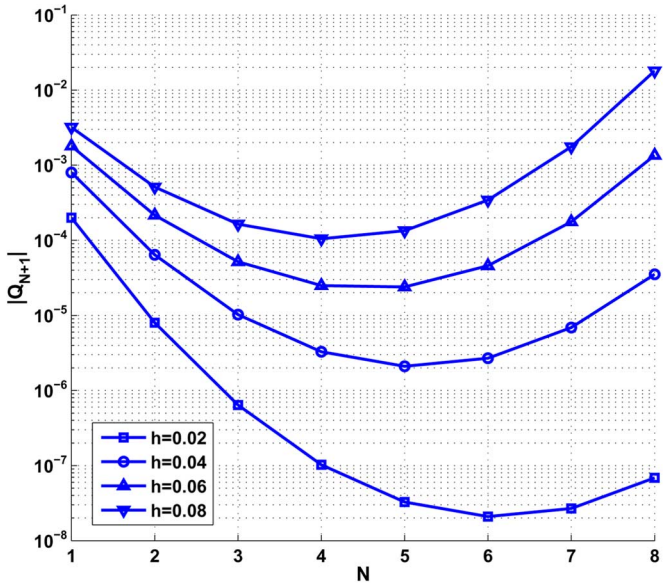

Fig. 6. $|Q_{N+1}|$ vs. N when $h = 0.02, 0.04, 0.06, 0.08$.

A. Simulation Example for the ESARE

Let us revisit the example of Section III-A. The numerical performance of the ESARE is depicted in Fig. 7. The accuracy of the ESARE is verified by showing the normalized reconstruction error with respect to N, as shown in Fig. 7(a). The maximum value of N for each h is determined such that $|Q_{N+1}|$ is minimized. The normalized reconstruction error is significantly decreased as N increases in spite of the fixed h, which could never be achieved by any previous inverse scattering methods. The accuracy improvement becomes larger for smaller h. Specifically, the normalized reconstruction error for $h = 0.08$ and $h = 0.02$ is reduced by up to a factor of 10^2 and 3×10^4, respectively. It can be seen from Fig. 7(a) that the accuracy improvement rate of the ESARE is decreased as N increases. In the case of $h = 0.02$, the accuracy of the 2-step ESARE compared to the 1-step ESARE is improved by a factor of 27, but the accuracy improvement is less than twice when N is increased from 4 to 5. Unlike the result of Section III, the performance of the ESARE is bounded by $N_{h,\max}$ due to the usage of the DSs which are larger than h. However, the discretization error of the 1-D CISP can be made negligible by the proposed ESARE, under relatively large h.

In the case of $h = 0.02$, the computational efficiency of the ESARE is shown in Fig. 7(b). The measure for the computational complexity is the number of multiplications. In Fig. 7(b), the complexity of the Schur algorithm is drawn such that the normalized reconstruction error is equivalent to that of the ESARE. While the complexity of the ESARE is almost stationary in spite of the decrease of the discretization error by a factor of 3×10^4, the complexity growth of the Schur algorithm amounts to a factor of 10^9. In our simulation, the runtime of the ESARE is less than one second, but the runtime of the Schur algorithm is larger than 18 days for the same performance with the 5-step ESARE.

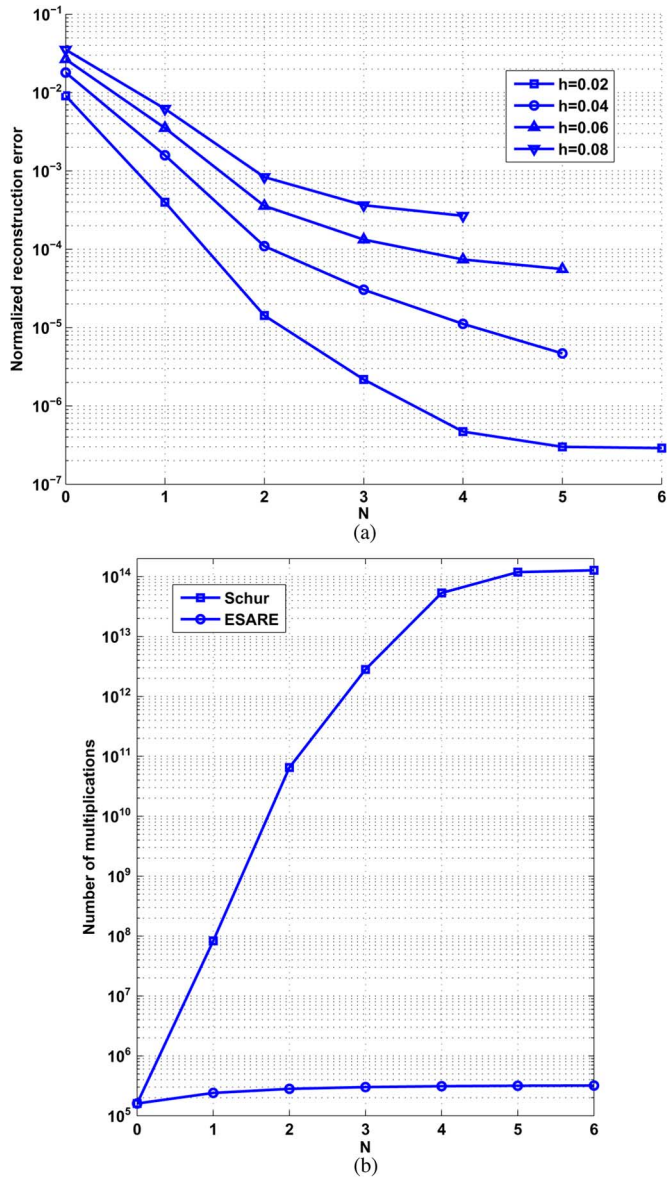

Fig. 7. Numerical performance of the ESARE: (a) normalized reconstruction error of the ESARE vs. N when $h = 0.02, 0.04, 0.06, 0.08$, (b) computational complexity of the ESARE and the Schur algorithm when $h = 0.02$.

V. Conclusion

We proposed the SARE to improve the accuracy or the complexity of the Schur algorithm for the 1-D CISP. Especially, the N-step ESARE achieved the accuracy $O(h^{N+1})$ with the complexity less than twice of the conventional Schur algorithm. Therefore, the ESARE decreases the discretization error of the Schur algorithm in a computationally efficient manner. One of our future works would be extension of the SARE to a higher dimensional ISP or lossy case.

References

[1] C. Mee, S. Seatzu, and D. Theis, "Structured matrix algorithms for inverse scattering on the line," *Calcolo*, vol. 44, no. 2, pp. 59–87, Dec. 2007.

[2] K. Case, "The discrete inverse scattering problem in one dimension," *J. Math. Phys.*, vol. 15, no. 2, pp. 143–146, Feb. 1974.

[3] P. M. Narayanan, P. Rulikowski, and J. Barrett, "Miniaturization of nonuniform transmission lines for ultra-wideband pulse shaping," in *Proc. IEEE COMCAS*, Tel-Aviv, Israel, 2011, pp. 1–6.

[4] L. S. Tamil and A. K. Jordan, "Spectral inverse scattering theory for inhomogeneous dielectric waveguides and devices," *Proc. IEEE*, vol. 79, no. 10, pp. 1519–1528, Oct. 1991.

[5] B. Gopinath and M. M. Sondhi, "Inversion of the telegraph equation and the synthesis of nonuniform lines," *Proc. IEEE*, vol. 59, no. 3, pp. 383–392, Mar. 1971.

[6] F. V. Comandini, M. Mirrahimi, and M. Sorine, "On the inverse scattering of star-shape LC-networks," in *Proc. IEEE CDC*, Cancun, Mexico, 2008, pp. 2075–2080.

[7] H. Tang and Q. Zhang, "An inverse scattering approach to soft fault diagnosis in lossy electric transmission lines," *IEEE Trans. Antennas Propag.*, vol. 59, no. 10, pp. 3730–3737, Oct. 2011.

[8] Q. Zhang, M. Sorine, and M. Admane, "Inverse scattering for soft fault diagnosis in electric transmission lines," *IEEE Trans. Antennas Propag.*, vol. 59, no. 1, pp. 141–148, Jan. 2011.

[9] J. A. Ware and K. Aki, "Continuous and discrete inverse scattering problems in a stratified elastic medium. I. Planewaves at normal incidence," *J. Acoust. Soc. Amer.*, vol. 45, no. 4, pp. 911–921, 1969.

[10] L. Amundsen, A. Reitan, H. K. Helgesen, and B. Arntsen, "Data-driven inversion/depth imaging derived from approximations to one-dimensional inverse acoustic scattering," *Inverse Problems*, vol. 21, no. 6, pp. 1823–1850, Dec. 2005.

[11] E. A. Robinson, "Dynamic predictive deconvolution," *Geophys. Prospect.*, vol. 23, pp. 779–797, Dec. 1975.

[12] A. M. Bruckstein, B. Levy, and T. Kailath, "Differential methods in inverse scattering," *SIAM J. Appl. Math.*, vol. 45, no. 2, pp. 312–335, Apr. 1985.

[13] A. M. Bruckstein and T. Kailath, "Inverse scattering for discrete transmission-line models," *SIAM Rev.*, vol. 29, no. 3, pp. 359–389, Sep. 1987.

[14] T. Kailath, "Signal processing applications of some moment problems," in *Proc. Symp. Appl. Math.*, 1987, vol. 37, pp. 71–109.

[15] T. Kailath, "A theorem of I. Schur and its impact on modern signal processing," *Operator Theory, Adv. Appl.*, vol. 18, pp. 9–30, 1986.

[16] I. Schur, "On power series which are bounded in the interior of the unit circle," *Operator Theory, Adv. Appl.*, vol. 18, pp. 31–59, 1986.

[17] I. M. Gelfand and B. M. Levitan, "On the determination of a differential equation from its spectral function," *Amer. Math. Soc. Transl.*, ser. 2, vol. 1, pp. 253–304, 1955.

[18] T. Kailath and A. H. Sayed, "Displacement structure: Theory and applications," *SIAM Rev.*, vol. 37, no. 3, pp. 297–386, Sep. 1995.

[19] S. Chandrasekaran and A. H. Sayed, "Stabilizing the generalized Schur algorithm," *SIAM J. Matrix Anal. Appl.*, vol. 17, no. 4, pp. 950–983, Oct. 1999.

[20] J. Chun and T. Kailath, "Divide-and-conquer solutions of least-squares problems for matrices with displacement structure," *SIAM J. Matrix Anal. Appl.*, vol. 12, no. 1, pp. 128–145, Jan. 1991.

[21] T. Kailath and J. Chun, "Generalized displacement structure for block-Toeplitz, Toeplitz-block, Toeplitz-derived matrices," *SIAM J. Matrix Anal. Appl.*, vol. 15, no. 1, pp. 114–128, Jan. 1994.

[22] J. Chun and T. Kailath, "Displacement structure for Hankel, Vandermonde, related (derived) matrices," *Linear Algebra Its Appl.*, vol. 151, no. 6, pp. 199–227, Jun. 1991.

[23] J. Chun and T. Kailath, "Fast parallel algorithms for QR and triangular factorization of structured matrices," *SIAM J. Sci. Stat. Comput.*, vol. 8, no. 6, pp. 899–913, Nov. 1987.

[24] J. Zhuang, W. Li, and A. Manikas, "Fast root-MUSIC for arbitrary arrays," *Electron. Lett.*, vol. 46, no. 2, pp. 174–176, Jan. 2010.

[25] A. H. Sayed and T. Kailath, "A survey of spectral factorization methods," *Numer. Linear Algebra Appl.*, vol. 8, no. 7, pp. 467–496, July 2001.

[26] K. Kim and J. Chun, "Convergence behavior of the Schur recursion in the Krein space for the J-spectral factorization," *IEEE Trans. Autom. Control*, vol. 10, pp. 1899–1903, Oct. 2000.

[27] T. T. Georgiou, "Computational aspects of spectral factorization and the tangential algorithm," *IEEE Trans. Circuits Syst.*, vol. 36, no. 1, pp. 103–108, Jan. 1989.

[28] Y. Choi, J. Bae, and J. Chun, "Numerically extrapolated discrete layer-peeling algorithm for synthesis of nonuniform fiber Bragg gratings," *Opt. Express*, vol. 19, no. 9, pp. 8254–8266, Apr. 2011.

[29] M. Chang, N. Kong, and P. Park, "Variable regularized least-squares algorithm: One-step-ahead cost function with equivalent optimality," *Signal Process.*, vol. 91, pp. 1224–1228, 2011.

[30] S. A. Samad, A. Hussain, and D. Isa, "Wave digital filters with minimum multiplier for discrete Hilbert transformer realization," *Signal Process.*, vol. 86, pp. 3761–3768, 2006.
[31] P. M. S. Burt and P. A. Regalia, "A new framework for convergence analysis and algorithm development of adaptive IIR filters," *IEEE Trans. Signal Process.*, vol. 53, no. 8, pp. 3129–3140, Aug. 2005.
[32] J. Bae, J. Chun, and T. Kailath, "The Schur algorithm applied to the design of optical multi-mirror structures," *Numer. Linear Algebra Appl.*, vol. 12, pp. 283–292, 2005.
[33] K. Maouche and D. T. M. Slock, "The fast subsampled-updating fast newton transversal filter (FSU FNTF) algorithm for adaptive filtering," *IEEE Trans. Circuits Syst. II*, vol. 47, no. 10, pp. 1047–1058, Oct. 2000.
[34] J. Chung and K. K. Parhi, "Pipelining of lattice IIR digital filters," *IEEE Trans. Signal Process.*, vol. 42, no. 4, pp. 751–761, Apr. 1994.
[35] S. K. Rao and T. Kailath, "Orthogonal digital filters for VLSI implementation," *IEEE Trans. Circuits Syst.*, vol. 31, no. 11, pp. 933–945, Nov. 1984.
[36] G. H. Song and S. Y. Shin, "Design of corrugated waveguide filters by the Gel'fan-Levitan-Marchenko inverse-scattering method," *J. Opt. Soc. Amer. A*, vol. 2, no. 11, pp. 1905–1915, Nov. 1985.
[37] I. Serban, F. Turcu, and M. Najim, "A fast 2-D AR parameter estimation algorithm based on functional Schur coefficients," *IEEE Signal Process. Lett.*, vol. 16, no. 12, pp. 1039–1042, Dec. 2009.
[38] I. Markovsky and S. Van Huffel, "Overview of total least-squares methods," *Signal Process.*, vol. 87, pp. 2283–2302, 2007.
[39] B. Li, Z. Liu, and L. Zhi, "A fast algorithm for solving the Sylvester structured total least squares problem," *Signal Process.*, vol. 87, pp. 2313–2319, 2007.
[40] Y. Chang and S. Chang, "A fast estimation algorithm on the Hurst parameter of discrete-time fractional Brownian motion," *IEEE Trans. Signal Process.*, vol. 50, no. 3, pp. 554–559, Mar. 2002.
[41] P. Dewilde and H. Dym, "Lossless inverse scattering, digital filters and estimation theory," *IEEE Trans. Infm. Theory*, vol. 30, no. 4, pp. 644–661, Jul. 1984.
[42] S. Wahls and H. Boche, "Realizable spatio-temporal Tomlinson-Harashima precoders: Theory and fast computation," *IEEE Trans. Signal Process.*, vol. 60, no. 9, pp. 4819–4833, Sep. 2012.
[43] C. B. Papadias, "Unsupervised receiver processing techniques for linear space-time equalization of wideband multiple input/multiple output channels," *IEEE Trans. Signal Process.*, vol. 52, no. 2, pp. 472–482, Feb. 2004.
[44] N. Al-Dhahir and A. H. Sayed, "The finite-length multi-input multi-output MMSE-DFE," *IEEE Trans. Signal Process.*, vol. 48, no. 10, pp. 2921–2936, Oct. 2000.
[45] M. Vollmer, M. Haardt, and J. Götze, "Comparative study of joint-detection techniques for TD-CDMA based mobile radio systems," *IEEE J. Sel. Areas Commun.*, vol. 19, no. 8, pp. 1461–1475, Aug. 2001.
[46] G. K. Kaleh, "Channel equalization for block transmission systems," *IEEE J. Sel. Areas Commun.*, vol. 13, no. 1, pp. 110–121, Jan. 1995.
[47] I. Serban and M. Najim, "Multidimensional systems: BIBO stability test based on functional Schur coefficients," *IEEE Trans. Signal Process.*, vol. 55, no. 11, pp. 5277–5285, Nov. 2007.
[48] M. Lopatka, O. Adam, C. L. J. Zarzycki, and J. Motsch, "Adaptative Schur algorithm dedicated to underwater transient signal processing," in *Proc. 149th Meeting of Acoust. Soc. Amer.*, 2005, p. 2493.
[49] I. Koltracht and P. Lancaster, "Threshold algorithms for the prediction of reflection coefficients in a layered medium," *Geophys.*, vol. 53, no. 7, pp. 908–919, Jul. 1988.
[50] W. Gragg, "On extrapolation algorithms for ordinary initial value problems," *J. SIAM Numer. Anal. Ser. B*, vol. 2, no. 3, pp. 384–403, 1965.
[51] L. F. Richardson, "The deferred approach to the limit. Part I. Single lattice," *Philos. Trans. Roy. Soc. London A*, vol. 226, pp. 299–361, Apr. 1927.
[52] D. C. Joyce, "Survey of extrapolation process in numerical analysis," *SIAM Rev.*, vol. 13, no. 4, pp. 435–490, Oct. 1971.

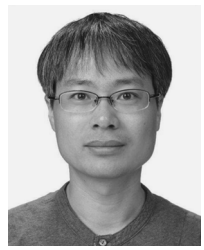

Youngchol Choi (M'12) received the double-major B.S. degree (*magna cum laude*) in electrical engineering and mathematics and M.S. and Ph.D. degrees in electrical engineering from the Korea Advanced Institute of Science and Technology (KAIST), Daejeon, Republic of Korea, in 1998, 2000, and 2011, respectively. Since 2000, he has been with the Korea Institute of Ocean Science and Technology (KIOST), Daejeon, Republic of Korea, where he is a Senior Research Scientist. His research interests include inverse scattering, MIMO systems, and ad-hoc network protocols for underwater acoustic communications.

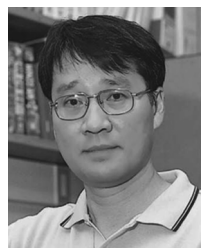

Joohwan Chun (S'82–M'94–SM'09) received the Ph.D. degree in electrical engineering from Stanford University, Stanford, CA, USA, in 1989. From 1989 to 1992, he was a member of the Technical Staff at General Electric, Schenectady, NY, USA. Since 1992, he has been a faculty member with the Department of Electrical Engineering, Korea Advanced Institute of Science and Technology (KAIST), Daejeon, Korea. He was a Visiting Professor with Stanford University from 1998 to 1999 and with the University of Toronto, ON, Canada, in 2006. His research interests include MIMO wireless communications and signal processing for radar systems. Dr. Chun has been an Associate Editor of the IEEE TRANSACTIONS ON VEHICULAR TECHNOLOGY since 2009.

Taejoon Kim (S'08–M'11) received the B.S. degree (with highest honors) from Sogang University, Korea and M.S. degree from the Korea Advanced Institute of Science and Technology (KAIST) both in electrical engineering in 2002 and 2004, respectively. From 2004 to 2006, he was with Electronics and Telecommunications Research Institute (ETRI), Korea. In 2007, he joined Purdue University, West Lafayette, Indiana and earned Ph.D. degree in Electrical and Computer Engineering in 2011. From 2011 to 2012, he was with the Nokia Research Center, Berkeley, California as a Senior Researcher. Before joining City University of Hong Kong in March 2013, he was a postdoctoral researcher in the Communication Theory group at KTH in Stockholm, Sweden. He was awarded the Korean government (MOCIE) scholarship for studying abroad in 2007 and the recipient of the Best Paper Award in IEEE PIMRC 2012. His research interests are in the design and analysis of communication systems and adaptive signal processing.

Jinho Bae received his Ph.D. degree from Korea Advanced Institute of Science and Technology (KAIST), Daejeon, Republic of Korea, in 2001. During 1993 and 2002, he was a member of the technical staff at Daeyang Electric Co., Busan, Republic of Korea. During 2006 and 2007, he was a visiting scholar of electrical and computer engineering department of Texas A&M University, Collage Station, TX, USA. Since 2002, he has been a faculty member in the Department of Ocean System Engineering at Jeju National University. His current research interests include optical filter design, layer peeling methods, and radar & sonar signal processing.